TASK QUARTERLY 8 No 4, 591–602

COMPUTER SIMULATION OF THE WORKING CYCLE OF A QUANTUM CONTROLLED-NOT GATE WITH TWO COUPLED QUANTUM DOTS

SŁAWOMIR MOSKAL, STANISŁAW BEDNAREK
AND JANUSZ ADAMOWSKI

Faculty of Physics and Nuclear Techniques,
AGH University of Science and Technology,
Al. Mickiewicza 30, 30-059 Cracow, Poland
gap@autograf.pl, {bednarek, adamowski}@novell.ftj.agh.edu.pl

(Received 6 June 2004)

Abstract: We discuss a possible realization of a quantum controlled-NOT gate with the use of two coupled quantum dots. Transitions between quantum states of a computational basis are driven by the microwave π-pulse. The parameters of the proposed nanodevice have been optimized in order to make the operation cycle of the gate as short as possible. Numerical solutions of the time-dependent Schrödinger equation allow us to simulate transitions between the quantum states which correspond to the subsequent stages of the gate's operation. The performed time-dependent simulations are a test of realizability of the quantum controlled-NOT gate in the nanodevice.

Keywords: semiconductor quantum dot, quantum gate operation, controlled-NOT (CNOT) gate

1. Introduction

In quantum computations [1], information is stored with quantum bits (qubits) and logical operations are performed on qubits with quantum logic gates. A single qubit can be represented by any two-level quantum system. Many-qubit states are constructed as tensor products of single-qubit states and are known as quantum registers [1].A quantum logic gate corresponds to the operation of a unitary transformation on a quantum register. There exists [2] a universal set of quantum logic gates which consists of all one-qubit gates and a single two-qubit gate, namely a controlled-NOT gate (CNOT). If we had a CNOT quantum gate at our disposal, we would approach a possible realization of a quantum computer.

The classical CNOT gate is presented in Figure 1, in which line aa' is called a control line because a logical state of this line decides about the state of the output of line bb', known as the target line. In the control line, the output state is always the same as the input state. The CNOT gate works like a NOT gate only if the control line is in logical state 1. In the opposite case, line bb' copies the input state to the

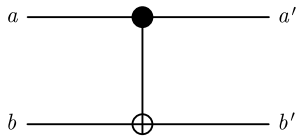

Figure 1. Scheme of the classical CNOT gate

a	b	a'	b'
0	0	0	0
0	1	0	1
1	0	1	1
1	1	1	0

Figure 2. Truth table of the CNOT gate

output, *i.e.* it does nothing. All the logical states of the CNOT gate are scheduled in the truth table shown in Figure 2.

Nowadays, physical realizations of the classical CNOT gate are reaching a natural limit of miniaturization, *i.e.* sizes of natural molecules. Even above this limit, *i.e.* for nanometer-sized electronic devices, quantum effects have become so strong that they can disturb the functionality of classical gates. However, we can directly exploit quantum effects to perform computations [1], which leads to the idea of a quantum computer [3]. The trend towards miniaturization is not the only reason of the recent interest in the physical realization of the quantum computer. It is expected that – due to the specific features of quantum systems – the future quantum computer should be more effective in some applications than present-day classical computers.

In the present paper, we study a possible physical realization of the quantum CNOT-gate model first proposed by Barenco *et al.* [4]. The model exploits the quantum states of two electrons in two coupled quantum dots. The single quantum dot (QD) is a nanostructure in which the electrons, confined in all three spatial dimensions, form localized states with discrete energy levels [5]. In this paper, we consider two QDs separated by a barrier layer. There are two crucial differences between classical and quantum logic gates. First, a classical electronic device contains physical input and output as well as physical wires, through which voltage signals are transmitted. In a quantum system, information is gathered in qubits. A qubit is represented by a quantum state vector in a two-dimensional Hilbert space, *i.e.*:

$$|\psi\rangle = \alpha|0\rangle + \beta|1\rangle, \tag{1}$$

where states $|0\rangle$ and $|1\rangle$ form a computational basis, and complex numbers α and β satisfy normalization condition $|\alpha|^2 + |\beta|^2 = 1$. In quantum computations, we will use the initial and final quantum states of the system as its input and output. Moreover, instead of voltage signals transmitted via wires, we will deal with a quantum evolution of the system.

The model of the CNOT gate studied in the present paper includes all the lowest-energy states of electrons confined in QDs. For a single electron confined in a single QD, these are the ground state (denoted by $|0\rangle$) and the first excited state (denoted by $|1\rangle$). For a system of two electrons confined in two weakly coupled QDs we

take into account ten subsequent lowest energy levels. The corresponding two-qubit states are constructed with the use of the following computational basis:

$$\{|00\rangle,|01\rangle,|10\rangle,|11\rangle\}, \tag{2}$$

where $|ij\rangle \equiv |i\rangle|j\rangle$ and $i,j=0,1$. The physical meaning of two-qubit basis states (2) is the following: state $|00\rangle$ describes a system in which each of the electrons occupies the single-particle ground state in a distinct QD, while in state $|01\rangle$ one of the electrons is in the ground state in the first QD and the other is in the first excited state in the second QD, *etc.* We assume throughout the present paper that QDs are formed by different asymmetric quantum wells [6]. Therefore, we can distinguish the control and target QD's. The profile of the potential confining the electrons in the z direction is shown in Figure 3. We will treat the left QD with the one-electron state $|i\rangle$ as the control QD (c) and the right QD with the one-electron state $|j\rangle$ as the target QD (t).

Using the operator formalism, the quantum CNOT logic gate is defined as follows [1]:

$$\begin{aligned}
\hat{U}_{\mathrm{CNOT}}|00\rangle &= |00\rangle,\\
\hat{U}_{\mathrm{CNOT}}|01\rangle &= |01\rangle,\\
\hat{U}_{\mathrm{CNOT}}|10\rangle &= |11\rangle,\\
\hat{U}_{\mathrm{CNOT}}|11\rangle &= |10\rangle,
\end{aligned} \tag{3}$$

where $\hat{U}_{\mathrm{CNOT}}$ is the unitary operator. Each operation given by Equations (3) has its counterpart in truth table (Figure 2).

An important difference between the classical and quantum CNOT gate follows from the quantum-mechanical superposition principle. According to this principle, the qubit (Equation (1)) defined as a superposition of the two different quantum states of the system is also the quantum state of the considered system. The superposition principle, together with the linearity of operator $\hat{U}_{\mathrm{CNOT}}$, can be applied to obtain the entangled state:

$$\hat{U}_{\mathrm{CNOT}}(\alpha|0\rangle+\beta|1\rangle)|0\rangle = \alpha|00\rangle+\beta|11\rangle. \tag{4}$$

In order to realize a quantum CNOT gate we need to find physical realizations of the computational basis and operator $\hat{U}_{\mathrm{CNOT}}$. A physical system ideal for this purpose is required to possess only four quantum states [4]. However, the real quantum world is more complicated than that. The present paper deals with this problem.

2. Model of a quantum CNOT gate

We consider two electrons in three-dimensional, cylindrically symmetric nanostructure composed of two QDs fabricated from a GaAs/AlGaAs heterostructure. The GaAs-made QDs are separated by a AlGaAs barrier layer, which is so thick that electron tunneling can be neglected. We assume that the lateral confinement potential, *i.e.* the potential in the $x-y$ plane, is much greater than the vertical confinement potential, *i.e.* the potential in the z direction, and can be approximated by the harmonic-oscillator potential. Then, the three-dimensional problem can be reduced to

a one-dimensional problem with the effective electron-electron interaction potential energy given by [7]:

$$U_{eff}(z_1,z_2)=\frac{e^2\sqrt{\pi\beta}}{4\pi\epsilon_0\epsilon}e^{\beta|z_1-z_2|^2}\operatorname{erfc}(\sqrt{\beta}|z_1-z_2|), \tag{5}$$

where ϵ_0 is the electric permittivity of vacuum, ϵ is the relative electric permittivity of GaAs, $\beta=m_e\omega_\perp/2\hbar$, m_e is the effective electron band mass, and $\hbar\omega_\perp$ is the excitation energy in the lateral harmonic-oscillator confinement potential. Therefore, each electron is described by only one spatial coordinate. Hence, we deal with a two-particle system described by the Hamiltonian:

$$\hat{H}(z_1,z_2)=-\frac{\hbar^2}{2m_e}\left(\frac{\partial^2}{\partial z_1^2}+\frac{\partial^2}{\partial z_2^2}\right)+U(z_1)+U(z_2)+U_{eff}(z_1,z_2)+2\hbar\omega_\perp, \tag{6}$$

where $U(z_i)$ is the vertical confinement potential energy of the i^{th} electron.

The vertical confinement potential $U(z_i)$ is asymmetric and different for each of the QDs (*cf.* Figure 3). The asymmetry of $U(z_i)$ leads to the electron densities shown in Figure 3. For the ground state and the first excited state, the electron densities are shifted in directions opposite to those for the symmetric confinement potential. Therefore, the interaction energy between electrons confined in distinct QD's will depend on their quantum states. We note that this effect of asymmetry is equivalent to the effect of an external electric field. However, an application of electric field can cause an escape of electrons from QD's shallow potential wells. As a consequence of the asymmetry of the confinement potential, electron energy levels are altered and take on different values. This change plays a crucial role in the operation of the CNOT gate. In the following, we focus on two energy differences, $\Delta E_I=E_{00}-E_{01}$ and $\Delta E_{II}=E_{10}-E_{11}$, where E_{ij} denotes the energy of state $|ij\rangle$ of the computational basis (see Figure 5). Energy separations ΔE_I and ΔE_{II} should take on clearly different values, which allows for selective absorption of electromagnetic radiation. According to Heisenberg's uncertainty principle, the longer the transition time between given energy levels, the smaller the misfit between the transition energy and the photon energy. At the same time, the gate's working time should be as short as possible. This requirement results from the necessity of minimization of interaction with the environment. Interaction of quantum system with the environment leads to decoherence, which introduces random relative phases into the qubits, which – in turn – can destroy the output results. The time that passes till the moment when the system becomes completely perturbed, *i.e.* loses its phase coherence, is known as decoherence time. Therefore, the time of the gate's working cycle should be much shorter than its decoherence time.

The CNOT gate will operate properly only if the energy levels associated with the computational basis states are distinctly separated. In the present work, we have optimized the parameters of the nanodevice in order to make the working-cycle time as short as possible.

The CNOT-gate working process consists of three steps. In the first step, the electron system is prepared in the ground state $|00\rangle$ (this step is called relaxation). In the second step, we set up the quantum state of the control dot, which can be either

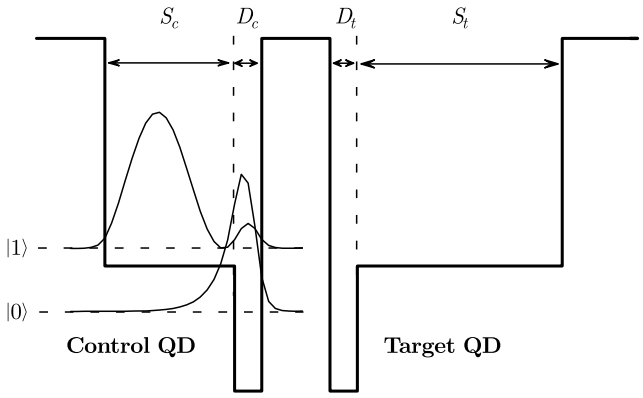

Figure 3. Vertical confinement potential and electron charge density for the ground state $|0\rangle$ (lower curve) and the first excited state $|1\rangle$ (upper curve) as functions of z; dashed lines show the ground-state and the first excited-state energy levels of a single electron confined in a single QD; the thicknesses of the shallow (deep) potential wells in the control and target QDs are denoted by $S_c(D_c)$ and $S_t(D_t)$, respectively

$|0\rangle$ or $|1\rangle$. In the last step, we simulate the action of the $\hat{U}_{\mathrm{CNOT}}$ operator and analyze the output state.

3. Parameters of the nanodevice

The calculations have been performed with the material parameters of GaAs, *i.e.* $m_e = 0.067 m_{e0}$, $\epsilon = \epsilon_\infty = 11$, where m_{e0} is the free electron mass, and ϵ_∞ is the high-frequency relative electric permittivity. We have optimized the other parameters of the nanodevice in order to obtain simulated operation of the CNOT gate with high fidelity. For this purpose, the electron-electron interaction should be strong for transition energies ΔE_I and ΔE_{II} to be distinctly separated. The interelectron interaction energy can be increased by either applying stronger lateral confinement or decreasing the distance between the electrons. The first condition is fulfilled if lateral confinement energy of $\hbar\omega_\perp = 40\,\mathrm{meV}$ is achieved, which is a rather large value, but technologically accessible. In order to decrease the distance between the electrons, we can decrease either the width of the barrier layer or the QD sizes. However, the barrier layer cannot be too small, since we want to neglect the tunneling effects.

In the states of our computational basis (2), electrons are fully localized in the QDs, thus allowing us to distinguish between the control and target QD. As the QD sizes in the z direction decrease, the energy separation between the ground and the first excited state increases. If this separation exceeds $\hbar\omega_\perp$, excitations between the states of the lateral confinement potential have to be included, which can disturb the gate's performance. We have taken this requirement into account by choosing the widths of the deep potential-well regions $D_c = D_t = 4\,\mathrm{nm}$ for both QDs and the widths of the shallow potential-well regions (S_c and S_t) large enough for the energy split to be less than $\hbar\omega_\perp$. The different values of widths S_c and S_t for the two QDs lead to splitting of energy levels E_{01} and E_{10}, which are associated with states $|01\rangle$ and $|10\rangle$, respectively. When setting the potential-well depths in regions $S_{c,t}$ and $D_{c,t}$, we have required the ground-state energy level to be located close to the shallow potential-well

bottom and the electron density to be localized in region $D_{c,t}$ for the ground state and in region $S_{c,t}$ for the first excited state (*cf.* Figure 3).

Taking into account all the above-mentioned physical aspects, we optimized the model nanodevice so that transition energies ΔE_I and ΔE_{II} were considerably different, expecting to obtain short-time operation cycles of the gate. The values of nanodevice parameters, for $\Delta E_I - \Delta E_{II} = 1.46\,\text{meV}$, are listed in Table 1.

Table 1. Parameters of the nanostructure used in the simulations

	width [nm]	depth [meV]
S_c	19	200
D_c	4	310
barrier	10	0
S_t	4	310
D_t	25	200

4. Numerical method

We calculate the two-electron eigenstates of Hamiltonian (6) using the imaginary time step method [8]. According to this method, we replace the derivatives in the time-dependent Schrödinger equation:

$$i\hbar\frac{\partial\psi}{\partial t}(z_1,z_2,t) = \hat{H}\psi(z_1,z_2,t), \tag{7}$$

with their finite-difference approximations and time by the pure imaginary variable $t = i\tau$. After simple transformations [8], we obtain the following equation:

$$\psi^{n+1} = \psi^n - \frac{\Delta\tau}{\hbar}\hat{H}\psi^n, \tag{8}$$

which can be used to find the ground-state wave function. The energy of this state is found as the expectation value of Hamiltonian $\hat{H}$. Superscript n in Equation (8) labels the subsequent iterations. Step $\Delta\tau$ has been chosen so that the procedure is as fast and stable as possible. The excited-state wave functions are found using the same method, complemented with orthogonalization to lower-energy wave functions.

The real-time evolution of the system has been realized using the iterative method, which is symmetric with respect to inversion in time [9]:

$$\psi^{n+1} = \psi^{n-1} - \frac{i}{\hbar}\Delta t\hat{H}'\psi^n. \tag{9}$$

In Equation (9), Hamiltonian $\hat{H}' = \hat{H} + \hat{H}_{int}$ includes operator $\hat{H}_{int}$ of the interaction of the electron system with radiation. Explicitly:

$$\hat{H}_{int}(z_1,z_2) = A\cos(\omega t)\hat{p} = -i\hbar A\cos(\omega t)\left(\frac{\partial}{\partial z_1} + \frac{\partial}{\partial z_2}\right), \tag{10}$$

where A is the amplitude of the radiation field, ω is the radiation's frequency, and $\hat{p}$ is the total momentum operator.

5. Results and discussion

The eigenfunctions of Hamiltonian (6) depend on two coordinates, z_1 and z_2. According to the probabilistic interpretation of quantum mechanics, the square

of the absolute value of the wave function, $|\psi(z_1,z_2)|^2$, represents the density of the probability that one of the electrons is placed in z_1 and the other in z_2. The probability density, calculated for the ten lowest-energy states, is shown in Figure 4. The corresponding ten lowest-energy levels are listed in Table 2 and shown in Figure 5. In Figure 4 and Table 2, we have introduced number ν, which numbers the states according to the increasing energy. We can treat ν as a convenient quantum number. In the states chosen as the states of the computational basis (2), electrons should be localized in different QDs. It can be seen in Figure 4 that this condition is satisfied only for the states with quantum numbers $\nu = 1,4,6,8,10$. However, the state with $\nu = 8$ does not belong to the computational basis selected in the present model, since in this state the electron in the control dot is in the ground state and the electron in the target dot is in the second excited state. Table 2 enables us to find the correspondence between the states numbered by ν and the states of the computational basis (2).

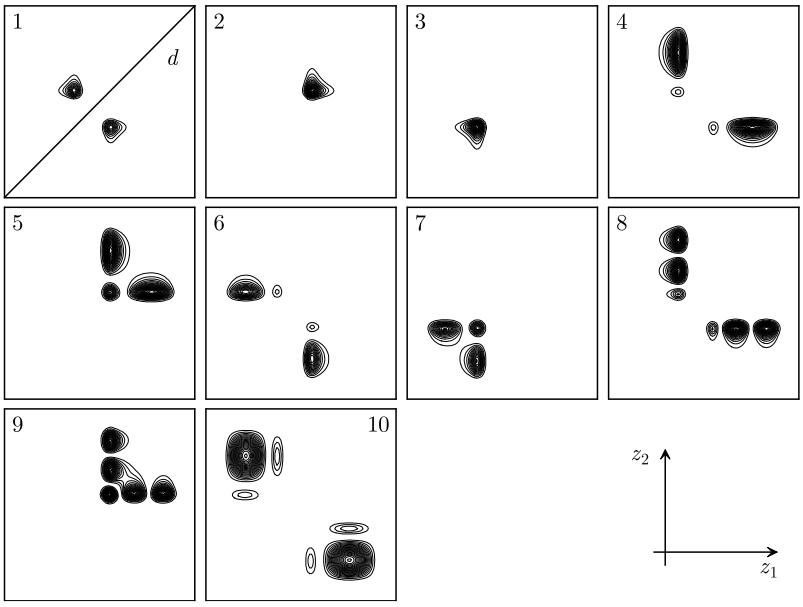

Figure 4. Contours of the two-electron probability density for the first ten lowest-energy states on plane $z_1 - z_2$; d denotes the diagonal

The probability density is symmetric with respect to the interchange of the electron coordinates, *i.e.* $|\psi(z_1,z_2)|^2 = |\psi(z_2,z_1)|^2$. This symmetry is equivalent to the reflection symmetry with respect to diagonal d in Figure 4. It is inconvenient to interpret two-particle densities; therefore, in Figure 6, we present one-particle densities defined as follows:

$$\rho_1(z_1) = \int_{-\infty}^{\infty} dz_2 |\psi(z_1,z_2)|^2. \tag{11}$$

The present approach yields a richer energy spectrum of the two-electron system than that used in the simple model [4]. The extra energy levels associated with states $\nu = 2,3,5,7,8,9,\ldots$ could in practice inhibit proper execution of the gate due

Table 2. (a) Lowest eigenvalues of Hamiltonian (6), computation-basis states are listed in the third column; (b) transition energies between the computational basis states

(a)

ν	energy [meV]	$\|ij\rangle$
1	-362.33	$\|00\rangle$
2	-347.63	
3	-347.56	
4	-331.45	$\|01\rangle$
5	-326.13	
6	-324.75	$\|10\rangle$
7	-317.44	
8	-306.50	
9	-299.43	
10	-292.40	$\|11\rangle$

(b)

energy difference	[meV]
$E_{01} - E_{00}$	30.89
$E_{11} - E_{10}$	32.35
$E_{10} - E_{01}$	6.7
$E_{10} - E_{00}$	37.59
$E_{11} - E_{01}$	39.04

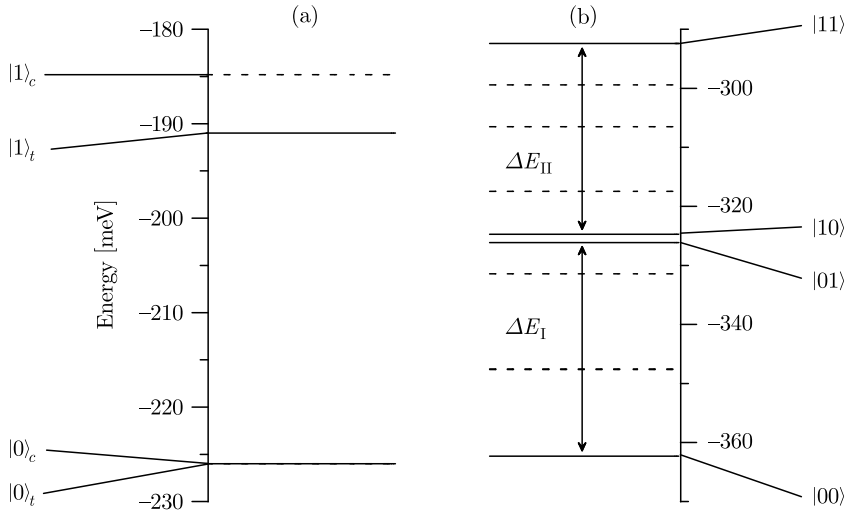

Figure 5. Energy levels of (a) one-qubit and (b) two-qubit states. $|0\rangle_{c,t}$ and $|1\rangle_{c,t}$ denote the ground and the first excited states of the electron in the control and target QDs, respectively; in (b), the most relevant energy separations are shown by arrows

to the increasing probability of unwanted transitions. Therefore, we have chosen the parameters of the nanodevice so that transitions to these states are less probable.

Transitions between the states of the computational basis, which form the operation cycle of the CNOT gate, are induced by the interaction of the electron system with radiation. These transitions will occur with probabilities close to 1 if the time of interaction is determined precisely. The interaction time is defined by the expression $A\langle\psi_{in}|\hat{p}|\psi_{fin}\rangle t = \pi$, where $|\psi_{in}\rangle$ and $|\psi_{fin}\rangle$ denote the initial state (before the transition) and the final state (after the transition), respectively. A radiation pulse with such a duration time is known as a π-pulse.

We have simulated the behaviour of a single electron in a single QD interacting with radiation. The photon energy has been matched to the energy difference between

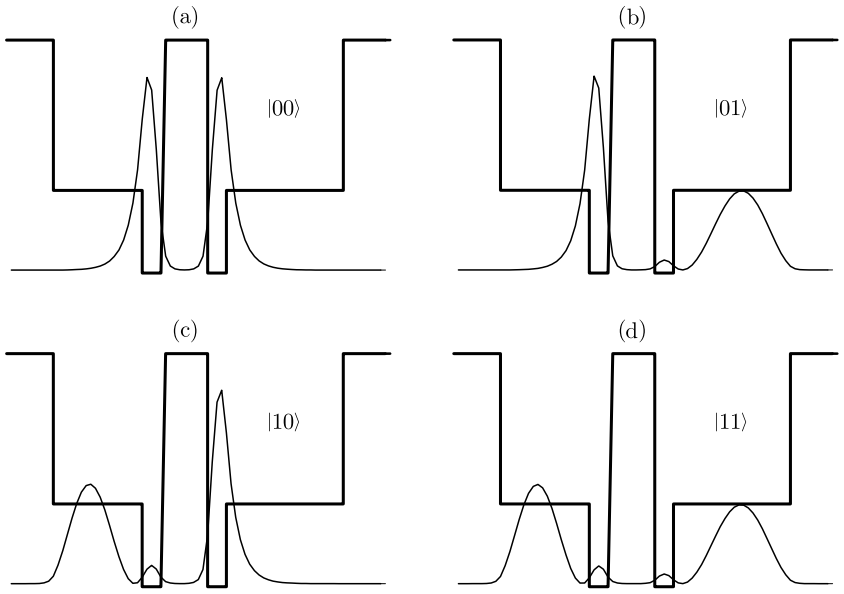

Figure 6. One-particle electron probability densities (Equation (11)) corresponding to the four states of the computational basis and the vertical confinement potential as functions of z; coordinate z varies in the horizontal direction

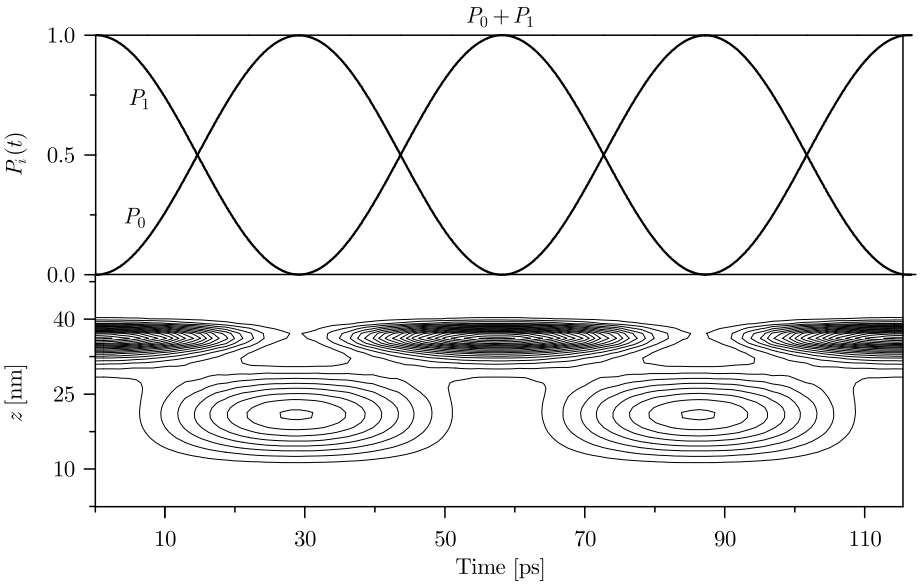

Figure 7. Time evolution of the one-electron probability density (Equation (11)) and the corresponding Rabi oscillations of probability $P_i(t)$

the ground and the first excited state. Figure 7 shows the calculated time evolution of the one-electron probability density (Equation (11)). We have also plotted in Figure 7 probability $P_i(t) = |\langle\psi_i|\psi(t)\rangle|^2$, where $|\psi(t)\rangle$ is the time-evolving state and the i subscript denotes the initial state. The lower panel of Figure 7 shows that

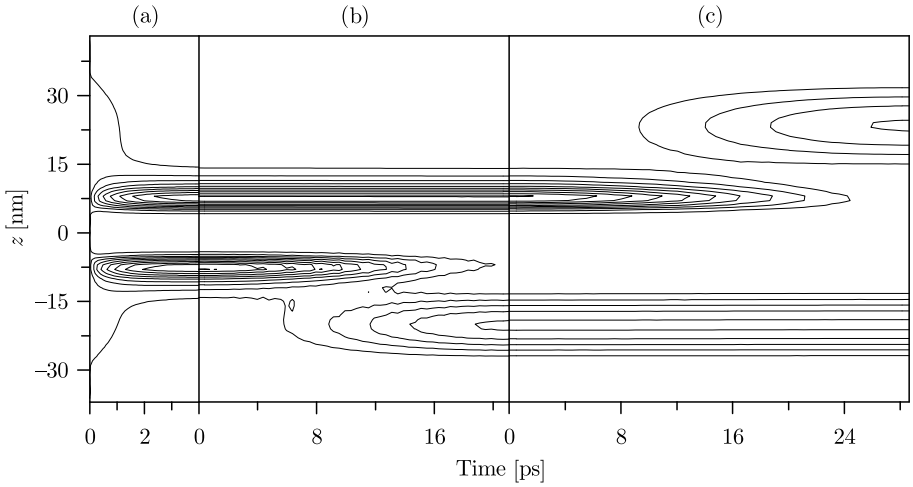

Figure 8. Working cycle of the CNOT gate when the control dot is prepared in state $|1\rangle$: (a) the relaxation step, (b) preparation of the control dot, (c) simulation of the $\hat{U}_{\mathrm{CNOT}}$ operation; as a result, the output qubit is changed

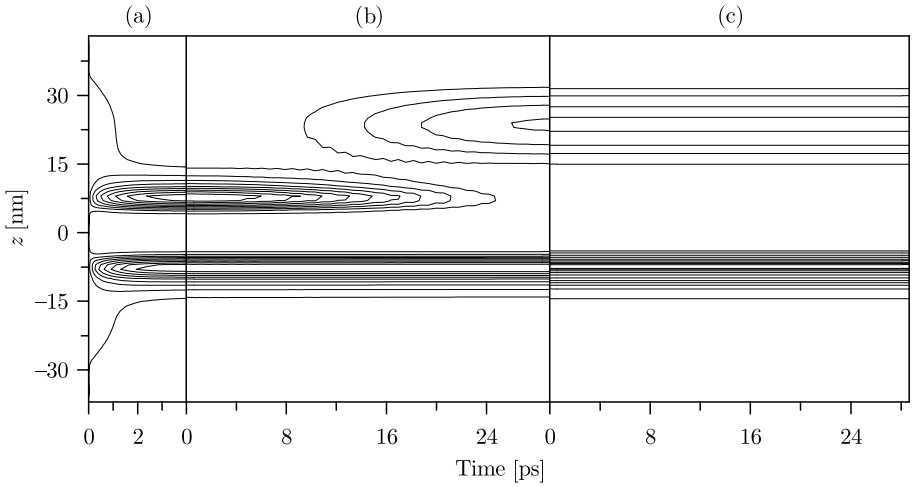

Figure 9. Working cycle of the CNOT gate when the control dot is prepared in state $|0\rangle$: (a) the relaxation step, (b) preparation of the control dot, (c) simulation of the $\hat{U}_{\mathrm{CNOT}}$ operation; as a result, the output qubit is unchanged

electron density oscillates between the S and D regions of the QD, *i.e.* between the $|0\rangle$ and $|1\rangle$ states. If the interaction with radiation is not terminated, the system will oscillate between these two states for an infinitely long time. This effect is known as Rabi oscillations.

The full working cycle of the gate operation is presented in Figures 8 and 9 in the form of contour plots of the one-electron probability density, $\rho_1(z_1,t)$. Simulation results are shown for the two chosen settings of the control QD. In Figures 8 and 9, the time evolution of the probability density illustrates the quantum transitions between the states of the computational basis. The stationary one-electron probability densities of the states involved are displayed in Figure 6. We start each gate operation cycle

with a relaxation of the system to the ground state. This relaxation process is realized with the help of the imaginary time step method. Only a few iterations are needed to prepare the ground state in which one of the electrons is localized in region D_c and the other – in region D_t (*cf.* Figure 3). The simulation of the relaxation is depicted in Figures 8a and 9a.

In the second step, we prepare the state of the control QD. For this purpose, we simulate the transitions from the ground state to either state $|10\rangle$ (Figure 8b) or state $|01\rangle$ (Figure 9b). These transitions are induced by the π-pulse of the electromagnetic wave with the frequency fitted to the corresponding transition energy. In the first simulated process (*cf.* Figure 8b), we can observe that the one-electron probability density in the control dot is transferred from region D_c to region S_c, which corresponds to the transition of an electron from the ground state to the first excited state. In the target dot, however, the one-electron probability density remains unchanged, which means that this QD remains in its ground state. In the other case (*cf.* Figure 9b), a different process is simulated: the electron in the target dot is pumped to the first excited state and the electron in the control dot remains in the ground state.

After preparing the control dot state, we apply the π-pulse with frequency adjusted to the $|10\rangle \longleftrightarrow |11\rangle$ transition, which realizes the $\hat{U}_{\mathrm{CNOT}}$ operation. Figure 8c shows that – as a result of this operation – the electron in the target dot is transformed from the ground state to the first excited state, while the electron in the control dot remains undisturbed. However, if we prepare the system in the $|01\rangle$ state, the same π-pulse has no effect, as illustrated in Figure 9c. We have thus simulated the working cycle of the CNOT gate with a system of two coupled QDs and two electrons.

The durations of the relevant transitions depend on the amplitude of the electromagnetic wave: the larger the amplitude, the faster the transition. Nevertheless, the energetic selectivity of the transitions decreases. For the energy separation of $\Delta E_I - \Delta E_{II} = 1.46\,\mathrm{meV}$, we have chosen a value of the electromagnetic-wave amplitude, for which the occupation probabilities, P_i, reach 1 (0) with the fidelity level of not less than 99.6%. According to the theory, 100% fidelity is reached in the limit of infinite time of interaction with radiation at an infinitesimaly small radiation amplitude. The estimated durations of different transitions for the required fidelity are given in Table 3.

Table 3. Estimated duration of microwave π-pulses for different transitions

transition	time [ps]
$\|00\rangle - \|01\rangle$	29.0
$\|00\rangle - \|10\rangle$	21.1
$\|10\rangle - \|11\rangle$	28.6

The decoherence time for GaAs QDs is $\sim 1000\,\mathrm{ps}$ [4], in our simulation, the total time of setting the control QD and performing the CNOT operation is estimated to be 49.7ps for the first process (Figure 8) and 57.7ps for the second process (Figure 9). This means that we can execute less than ~ 20 operation cycles before decoherence destroys the qubits. In order to obtain a shorter π-pulse duration in the subsequent steps of the operation cycle, it is necessary to increase the differences between the

energy levels associated with the states of the computational basis. It will then be possible to increase the amplitude of the electromagnetic wave, which will drive faster transitions.

In summary, the present results suggest that the construction of a quantum CNOT gate with the use of two coupled QDs is difficult to realize in practice. Our simulations have shown that the modeled CNOT gate can operate, however, its working cycle must be shortened if it is to become an effective element of a solid-state quantum computer.

Acknowledgements

This work has been partly supported by the Polish Ministry for Scientific Research and Information Technology under solicited grant no. PBZ-MIN-008/P03/2003.

References

[1] Nielsen M A and Chuang I L 2000 *Quantum Computation and Quantum Information*, Cambridge University Press, UK
[2] Barenco A, Benett C H, Cleve R, DiVincenzo D P, Margolus N, Shor P, Sleator T, Smolib J A and Weinfurter H 1995 *Phys. Rev.* **A 52** 3457
[3] Feynman R P 1986 *Foundations of Physics* **16** 507
[4] Barenco A, Deutsch D, Eckert A and Jozsa R 1995 *Phys. Rev. Lett.* **74** 4083
[5] Jacak L, Hawrylak P and Wójs A 1998 *Quantum Dots*, Springer-Verlag, Berlin
[6] Sanders G D, Kim K W and Holton W C 2000 *Phys. Rev.* **B 61** 7526
[7] Bednarek S, Szafran B, Chwiej T and Adamowski J 2003 *Phys. Rev.* **B 68** 045328
[8] Davies K T R, Flocard H Krieger S and Weiss M S 1980 *Nucl. Phys.* **A 342** 111
[9] Askar A and Cakmak A S 1978 *J. Chem. Phys.* **68** 2794